Andreev reflection in normal metal/charge-4*e* superconductor junctions

Yi-Xin Dai [1,2] and Qing-Feng Sun [1,2,3,*]

[1]*International Center for Quantum Materials, School of Physics, Peking University, Beijing 100871, China*

[2]*Beijing Academy of Quantum Information Sciences, West Bld. #3, No. 10 Xibeiwang East Rd., Haidian District, Beijing 100193, China*

[3]*Hefei National Laboratory, Hefei 230088, China*

(Received 26 January 2024; revised 11 March 2024; accepted 19 March 2024; published 4 April 2024)

We investigate the Andreev reflection in a normal metal/charge-4*e* superconductor junction. Compared with the electron-hole conversion in normal charge-2*e* superconductors, here four electrons participate simultaneously, enriching the possibility of conversion ways. Using the nonequilibrium Green's function method, we obtain a four-particle-type Landauer-Büttiker formula with generalized charge-4*e* anomalous Green's function to describe it. We then calculate and clarify the behavior of the Andreev coefficient and the conductance contributed by it, showing features like the unconventional position of the peak structure and the emerging plateau inside the superconducting gap. Our research makes up the blank of research for transport property of charge-4*e* superconductors and can serve as a hallmark for future experimental verifications.

DOI: 10.1103/PhysRevB.109.144504

I. INTRODUCTION

Charge-4*e* superconductivity (charge-4*e* SC) names the condensate of the quartets of electrons. Such electron pairs can carry a charge of 4*e*, which differs from the normal charge-2*e* Cooper pairs described by the Bardeen-Cooper-Schrieffer theory [1]. It was proposed in a wide range of fields [2–9]. Especially in the theory of intertwined orders in cuprate superconductors, the charge-4*e* SC is described as a vestigial phase in the thermal melting of pair-density-wave order [10,11]. Recent progress in experiments makes charge-4*e* SC more attractive [12,13], due to the possible evidence for charge-4*e* and even charge-6*e* pairs in kagome superconductors. Although theorists have proposed a possible mechanism for charge-4*e*/6*e* pairs [14–16], it still requires more evidence to confirm the existence of charge-4*e* SC in experiments. Therefore, it is quite necessary to investigate the transport properties of charge-4*e* SC in the hope of giving more hallmarks to distinguish it from the perspective of transport phenomena.

The former researches are mainly focusing on the equilibrium properties of charge-4*e* SC [6–8,17–21]. By applying the theory of vestigial order and the Ginzburg-Landau method, they showed the appearance of charge-4*e* SC order and discussed the phase competition between it and other orders, such as pair-density-wave and nematic orders [9,18,19,22,23]. While those studies were phenomenological in general, some works began to pay attention to the microscopic mechanics of forming four-electron pairs [24–27]. A real-space mean-field Hamiltonian, in which four electrons on the neighboring sites can form a pair, was proposed with quantum Monte Carlo simulations revealing chemical potential controlled phase transition between charge-4*e* SC and charge-2*e* SC [25]. Using the solvable Sachdev-Ye-Kitaev model, a charge-4*e* superconductor with gapless ground state was also described [26]. Besides, similar to the BCS wave function for charge-2*e* SC, a charge-4*e* wave function with its corresponding mean-field Hamiltonian has also been proposed [27]. While this Hamiltonian describes a gapped charge-4*e* SC phase, it can also be seen as a natural extension of the theory of intertwined orders.

To study the transport with superconductors, one often encounters the interface between leads and superconductors. It is well known that an incident electron can be reflected as a hole at the interface between a normal metal and a superconductor, namely, the Andreev reflection. This process can convert the normal current into the supercurrent, governing the conductance of the interface below the superconducting gap. Moreover, as the incident electron and reflected hole can be regulated by both sides of the junction, the Andreev reflection is often used to reveal the novel properties of materials either in the normal side [28–31] or in the superconducting side [32–35]. Therefore, to understand the transport with charge-4*e* SC, it is natural to consider the possible Andreev reflection happening in the interface between a normal metal and a charge-4*e* superconductor. At this point, the conventional picture involving two participating electrons may be inapplicable due to the electron quartet, which introduces more freedom as well as complexity.

In this paper, we investigate the charge-4*e* Andreev reflection (charge-4*e* AR) in a normal metal/charge-4*e* superconductor junction. Due to the characteristics of quartet condensation, the Andreev reflection here involves four particles, enriching the possibility of conversion ways. Using nonequilibrium Green's function method, we derive a four-particle-type Landauer-Büttiker formula with generalized charge-4*e* anomalous Green's function to describe the Andreev reflection process. We then calculate and clarify the behavior of charge-4*e* AR with various incident energy and

*sunqf@pku.edu.cn

show the conductance contributed by it. We find that there exist features including the unconventional position of the peak structure and the emerging plateau inside the superconducting gap. Our results provide formulas and pictures to describe the charge-4*e* AR, which can enrich the understanding of the transport with charge-4*e* SC and give guidance for future experimental verifications.

The rest of the paper is as follows: In Sec. II, we give the Hamiltonian of the normal metal/charge-4*e* superconductor junction and derive the formula for the transport process. In Secs. III and IV, we calculate the Andreev coefficient using perturbation and nonperturbation methods, which characterize the Andreev reflection from different perspectives while maintaining some consistency. We then give the whole picture of charge-4*e* AR in Sec. V and further consider the conductance in Sec. VI. Finally, a summary is presented in Sec. VII.

II. MODEL AND FORMULA

We consider a normal metal/charge-4*e* superconductor junction, which is described by the following Hamiltonian $H_{\rm tot} = H_L + H_R + H_C$, with

$$\begin{aligned} H_L &= \sum_{i,k,\sigma} \epsilon_{L,ik}\, a^\dagger_{ik\sigma} a_{ik\sigma}, \\ H_R &= \sum_{i,k,\sigma} \epsilon_{R,ik}\, c^\dagger_{ik\sigma} c_{ik\sigma} + H_{\rm SC}, \\ H_C &= \sum_{i,k,k',\sigma} t_{Lk,Rk'}\, a^\dagger_{ik\sigma} c_{ik'\sigma} + \text{H.c.}, \end{aligned} \tag{1}$$

where H_L, H_R, and H_C represent the Hamiltonians of left lead (normal metal), right lead (charge-4*e* superconductor), and their coupling, respectively. $a_{ik\sigma}$ ($c_{ik\sigma}$) are electron annihilation operators in the left (right) lead, with k denoting the momentum and $\sigma = \uparrow, \downarrow$ denoting the electron spins. Besides, $\epsilon_{L/R,ik}$ and $t_{Lk,Rk'}$ are the energy dispersion and hopping strength. We set $t_{Lk,Rk'} = t_c$ below for convenience [36]. $H_{\rm SC}$ describes the superconducting interaction. Adopting the charge-4*e* mean-field Hamiltonian in Ref. [27] and introducing the index $i = 1, 2$ to fulfill the Pauli exclusion principle (like pair-density-wave order momentum, nematic order component, layer degree of freedom, etc. [7,8,10,15,37]), we have

$$H^{4e}_{\rm SC} = \Delta \sum_k (c^\dagger_{1k\uparrow} c^\dagger_{1-k\downarrow} c^\dagger_{2k\uparrow} c^\dagger_{2-k\downarrow} + \text{H.c.}), \tag{2}$$

with Δ being the superconducting pairing potential. To compare with the charge-2*e* SC, we also write the charge-2*e* Hamiltonian $H^{2e}_{\rm SC} = \Delta \sum_k (c^\dagger_{1k\uparrow} c^\dagger_{1-k\downarrow} + \text{H.c.})$ with the index $i = 1$ only.

Due to the symmetry of $H_{\rm tot}$, exchanging arbitrary two channels could exchange their currents while keeping $H_{\rm tot}$ unchanged. Therefore, the current of each channel must be equal, leading to a total current being four times that of a single channel. We thus consider the current flowing from channel $1\uparrow$ via the time derivative of electron number operator $N_{1\uparrow,L} = \sum_k a^\dagger_{1k\uparrow} a_{1k\uparrow}$ [38],

$$\begin{aligned} I_{1\uparrow} &= -e\langle \dot{N}_{1\uparrow,L} \rangle \\ &= \frac{ie}{h} \int \mathrm{d}\omega_1 \Gamma^L \big[f^e_{1\uparrow}(\omega_1) G^>_{1\uparrow}(\omega_1) + \bar{f}^e_{1\uparrow}(\omega_1) G^<_{1\uparrow}(\omega_1) \big], \end{aligned} \tag{3}$$

where $\Gamma^L = 2\pi \rho_L |t_c|^2$ with ρ_L being the density of states in the left lead. $\bar{f}^e_{1\uparrow}(\omega_1) = 1 - f^e_{1\uparrow}(\omega_1)$ and $f^e_{1\uparrow}(\omega_1) = f(\omega_1 - eV) = 1/[e^{(\omega_1 - eV)/k_B\mathcal{T}} + 1]$ is the Fermi distribution function of channel $1\uparrow$ in electron type with the bias voltage V and temperature $\mathcal{T}$. The less and greater Green's functions $G^{\lessgtr}_{1\uparrow}(\omega_1)$ are the Fourier transforms of $G^{\lessgtr}_{1\uparrow}(t, 0)$, which are defined as $G^<_{1\uparrow}(t, 0) = i \sum_{kk'} \langle c^\dagger_{1k'\uparrow}(0) c_{1k\uparrow}(t) \rangle$ and $G^>_{1\uparrow}(t, 0) = -i \sum_{kk'} \langle c_{1k\uparrow}(t) c^\dagger_{1k'\uparrow}(0) \rangle$. Equation (3) is a simple transform of the usual Landauer formula [39] and contains all the possible transport processes of an interacting system.

A. Andreev reflection in charge-2*e* SC

Before starting our procedure in calculating charge-4*e* AR, we first briefly review the Andreev reflection in charge-2*e* SC. To describe charge-2*e* AR, we need to explicitly insert the coupling term of channel $1\downarrow$ into the nonequilibrium Green's function $G_{1\uparrow,k_1k'_1}(\tau_1, \tau'_1) = -i\langle c_{1k_1\uparrow}(\tau_1) c^\dagger_{1k'_1\uparrow}(\tau'_1) \rangle^c$, with superscript "$c$" denoting the complex contour time order and the time τ_1 and τ'_1 being defined on the contour [40], to do the perturbation expansion. This would introduce the nonequilibrium anomalous Green's functions $F_{k_1k_2}(\tau_1, \tau_2) = -i\langle c_{1k_1\uparrow}(\tau_1) c_{1-k_2\downarrow}(\tau_2) \rangle^c$ and $F^\dagger_{k'_2k'_1}(\tau'_2, \tau'_1) = -i\langle c^\dagger_{1-k'_2\downarrow}(\tau'_2) c^\dagger_{1k'_1\uparrow}(\tau'_1) \rangle^c$. After applying the analytic continuation and Fourier transform, we derive the part of the $G^{\lessgtr}_{1\uparrow}(\omega_1)$ relating to the process of Andreev reflection (denoted with subscript "A") as

$$\begin{aligned} G^>_{1\uparrow,A}(\omega_1) &= F^r(\omega_1) \big[-i \bar{f}^h_{1\downarrow} \Gamma^L \big] F^{\dagger,a}(\omega_1), \\ G^<_{1\uparrow,A}(\omega_1) &= F^r(\omega_1) \big[i f^h_{1\downarrow} \Gamma^L \big] F^{\dagger,a}(\omega_1), \end{aligned} \tag{4}$$

where $\bar{f}^h_{1\downarrow} = 1 - f^h_{1\downarrow}$ and $f^h_{1\downarrow} = f(\omega_1 + eV)$ is the Fermi distribution function of channel $1\downarrow$ in hole type. $F^r(\omega_1)$ and $F^{\dagger,a}(\omega_1)$ are the Fourier transforms of $\sum_{k_1k_2} F^r_{k_1k_2}(t, 0)$ and $\sum_{k'_2k'_1} F^{\dagger,a}_{k'_2k'_1}(t, 0)$. The retarded (advanced) Green's functions can be obtained from the analytic continuation

$$\begin{aligned} F^r(t_1, t_2) &= F\big(t_1^s, t_2^+\big) - F\big(t_1^s, t_2^-\big), \\ F^{\dagger,a}(t_2, t_1) &= F^\dagger\big(t_2^+, t_1^s\big) - F^\dagger\big(t_2^-, t_1^s\big), \end{aligned} \tag{5}$$

with $s = +$ or $-$. The arbitrary choosing of $s = \pm$ branch of the complex contour shows the causality [41] that $t_1 > t_2$ in $F^r(t_1, t_2)$ and $F^{\dagger,a}(t_2, t_1)$. Substituting Eq. (4) into (3), we obtain the current contributed by the Andreev reflection

$$I_{1\uparrow,A} = \frac{e}{h} \int \mathrm{d}\omega_1 \big(f^e_{1\uparrow} \bar{f}^h_{1\downarrow} - \bar{f}^e_{1\uparrow} f^h_{1\downarrow} \big)\, T_A, \tag{6}$$

with $T_A(\omega_1) = \Gamma^L F^r \Gamma^L F^{\dagger,a}$ being the Andreev reflection coefficient. Notice that $f^e_{1\uparrow} \bar{f}^h_{1\downarrow} - \bar{f}^e_{1\uparrow} f^h_{1\downarrow} = f^e_{1\uparrow} - f^h_{1\downarrow}$, so the Andreev reflection current in Eq. (6) is identical with that in

the literature [38,42,43]. For completeness, we leave the detailed derivation and the formula for other transport processes contributed to the total current in Appendix A 1.

B. Andreev reflection in charge-4*e* SC

It is then straightforward to generalize the charge-2*e* AR to the charge-4*e* AR. By inserting the coupling terms of the other three channels, we introduce the nonequilibrium charge-4*e* anomalous Green's function

$$\begin{aligned} &F_{k_1k_2k_3k_4}(\tau_1,\tau_2,\tau_3,\tau_4)\\ &\quad=-i\langle c_{1k_1\uparrow}(\tau_1)c_{1-k_2\downarrow}(\tau_2)c_{2k_3\uparrow}(\tau_3)c_{2-k_4\downarrow}(\tau_4)\rangle^c,\\ &F^\dagger_{k_4k_3k_2k_1}(\tau_4,\tau_3,\tau_2,\tau_1)\\ &\quad=-i\langle c^\dagger_{2-k_4\downarrow}(\tau_4)c^\dagger_{2k_3\uparrow}(\tau_3)c^\dagger_{1-k_2\downarrow}(\tau_2)c^\dagger_{1k_1\uparrow}(\tau_1)\rangle^c. \end{aligned} \tag{7}$$

After applying the analytic continuation and the Fourier transform, we obtain the part of the $G^{\lessgtr}_{1\uparrow}(\omega_1)$ relating to the process of charge-4*e* AR as

$$\begin{aligned} G^{>}_{1\uparrow,A}(\omega_1)&=-i\int_{234}F^r\left[\bar f^h_{1\downarrow}(\omega_2)\bar f^h_{2\uparrow}(\omega_3)\bar f^h_{2\downarrow}(\omega_4)(\Gamma^L)^3\right]F^{\dagger,a},\\ G^{<}_{1\uparrow,A}(\omega_1)&=i\int_{234}F^r\left[f^h_{1\downarrow}(\omega_2)f^h_{2\uparrow}(\omega_3)f^h_{2\downarrow}(\omega_4)(\Gamma^L)^3\right]F^{\dagger,a}, \end{aligned} \tag{8}$$

where $\bar f^h_{i\sigma}(\omega)=1-f^h_{i\sigma}(\omega)$ and $f^h_{i\sigma}(\omega)=f(\omega+eV)$ is the Fermi distribution function of channel $i\sigma$ in hole type. The integral $\int_{234}$ represents the energy convolution $\int d\omega_2 d\omega_3 d\omega_4\delta(\omega_1-\omega_2-\omega_3-\omega_4)/4\pi^2$, constraining the total energy of the three reflected holes to form four-electron pairs at the Fermi surface. $F^r=F^r(\omega_2,\omega_3,\omega_4)$ and $F^{\dagger,a}=F^{\dagger,a}(\omega_4,\omega_3,\omega_2)$ are the Fourier transforms of $\sum_{k_i}F^r_{k_1k_2k_3k_4}(0,t_2,t_3,t_4)$ and $\sum_{k'_j}F^{\dagger,a}_{k'_4k'_3k'_2k'_1}(t_4,t_3,t_2,0)$, respectively. We have the generalized retarded (advanced) Green's functions (omitting the momentum index for simplification)

$$\begin{aligned} F^r(t_1,t_2,t_3,t_4)&=\sum_{s_2s_3s_4}(-1)^PF\left(t_1^\pm,t_2^{s_2},t_3^{s_3},t_4^{s_4}\right),\\ F^{\dagger,a}(t_4,t_3,t_2,t_1)&=\sum_{s_2s_3s_4}(-1)^PF^\dagger\left(t_4^{s_4},t_3^{s_3},t_2^{s_2},t_1^\pm\right), \end{aligned} \tag{9}$$

with $s_{2,3,4}=\pm$ being the branch index and P being the total number of "–" branches among them. Note that the results in Eq. (9) are the same regardless of t_1 either on + branch or on – branch. This arbitrary choosing of the branch of t_1 is protected by the causality that $t_1>t_2,t_3,t_4$.

Substituting Eq. (8) into (3) leads to a four-particle Landauer formula

$$I_{1\uparrow,A}=\frac{e}{h}\int_{1234}\left(f^e_{1\uparrow}\bar f^h_{1\downarrow}\bar f^h_{2\uparrow}\bar f^h_{2\downarrow}-\bar f^e_{1\uparrow}f^h_{1\downarrow}f^h_{2\uparrow}f^h_{2\downarrow}\right)T_A, \tag{10}$$

with $\int_{1234}$ being $\int d\omega_1 d\omega_2 d\omega_3 d\omega_4\delta(\omega_1-\omega_2-\omega_3-\omega_4)/4\pi^2$ and

$$T_A(\omega_2,\omega_3,\omega_4)=\Gamma^LF^r(\Gamma^L)^3F^{\dagger,a} \tag{11}$$

being the charge-4*e* Andreev reflection coefficient. This is one of the central results of this work. It describes the charge-4*e* Andreev reflection process, where one incident electron can be reflected to three holes at the interface between normal metal and charge-4*e* superconductor (shown in Fig. 1), and can be easily extended to multielectron Andreev reflection. Note that since the Fermi distribution functions of electron and hole can be transformed by $\bar f^h_{i\sigma}(\omega^h)=f^e_{i\sigma}(\omega^e)$ with $\omega^e=-\omega^h$, the number of incident electrons and reflected holes just depends on the way we treat each channel as electron type or hole type. We thus can rewrite Eq. (10) as

$$I_{1\uparrow,A}=\frac{e}{h}\int'_{1234}\left(f^ef^ef^ef^e-\bar f^e\bar f^e\bar f^e\bar f^e\right)T_A, \tag{12}$$

omitting the channel index $i\sigma$. Here $\int'_{1234}$ denotes the energy integral $\int d\omega^e_1 d\omega^e_2 d\omega^e_3 d\omega^e_4\delta(\omega^e_1+\omega^e_2+\omega^e_3+\omega^e_4)/4\pi^2$ with $\omega^e_1=\omega_1$, $\omega^e_{2,3,4}=-\omega_{2,3,4}$ unifying the energy variables in electron type.

We then consider the conductance contributed by the charge-4*e* AR, which can be obtained from $G_A=\partial I_{1\uparrow,A}/\partial V$:

$$G_A=\frac{e^2}{h}\sum_{i=1}^{4}\int'_{1234-i}\left(f^ef^ef^e+\bar f^e\bar f^e\bar f^e\right)T_A|_{\omega^e_i=eV}, \tag{13}$$

assuming that T_A is independent of the voltage V. Here the integral $\int'_{1234-i}$ is over the other three energy variables while keeping $\omega^e_i=eV$. For completeness, we leave in Appendix A 2 the detailed derivation as well as the transport formula for other transport processes and their contributions to the total conductance. Recall that in charge-2*e* SC, G_A is simply proportional to T_A, the integral nature here would make the conductance of charge-4*e* SC quite different from that of charge-2*e* SC.

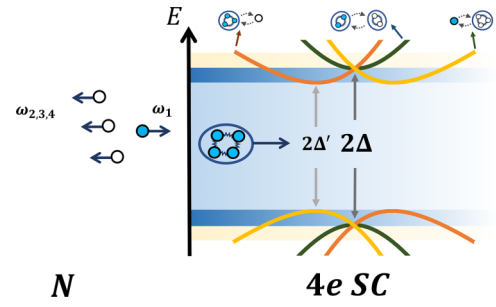

FIG. 1. Schematics of charge-4*e* Andreev reflection in the normal metal/charge-4*e* superconductor junction, where one incident electron carrying energy ω_1 can be reflected to three holes carrying energy $\omega_{2,3,4}$ at the interface of the junction, injecting a four-electron pair into the right side. The green, yellow, and orange lines show the energy dispersion of different types of quasiparticles in charge-4*e* SC. While the mixing of charge-2*e* particles (holes) owns a direct gap Δ, the mixing of charge-$e/3e$ particles (holes) owns an indirect gap $\Delta'=\sqrt{3}\Delta/2$.

III. PERTURBATION IN SUPERCONDUCTIVITY: LOWEST-ORDER EXPANSION

It is challenging to solve the charge-4*e* anomalous Green's functions $F, F^\dagger$ and give an exact form of T_A. Therefore, we begin our analysis by considering some specific conditions where perturbation theory can take effect.

We first consider expanding the Andreev reflection coefficient to the lowest order of charge-4e superconducting pairing potential Δ. Due to the many-body correlation nature of charge-4e SC, in the theoretical description, one usually has no particular reason to expect the charge-4e pairing potential to be weak enough to apply a perturbation theory [26]. However, such a challenge can be avoided in transport problems, as we investigate the state that the energy of the incident electron is much greater than the superconducting gap. Compared with the injecting energy, the pairing potential can now be seen as a small quantity, which makes the perturbation effective.

Therefore, we can expand the charge-4e anomalous Green's function to the lowest order of Δ and obtain the Andreev reflection coefficient up to Δ^2 order (here we also give the result of charge-2e SC for comparison),

$$T^{(1)}_{A,4e} = 4z^4 \frac{(\Delta/\pi\rho_R)^2}{(\omega_1+\omega_2)^2(\omega_1+\omega_3)^2(\omega_1+\omega_4)^2},$$
$$T^{(1)}_{A,2e} = 4z^2 \frac{\Delta^2}{(\omega_1+\omega_2)^2}, \tag{14}$$

with $z = \pi\rho_R\Gamma^L/(1+\pi\rho_R\Gamma^L/2)^2$ measuring the influence of coupling. Here ρ_R is the density of states in the right lead. We have energy constraint $\omega_2 = \omega_1$ for charge-2e SC and $\omega_2+\omega_3+\omega_4 = \omega_1$ for charge-4e SC, showing that the total energy carried by the reflected holes is equal to that of the incident electron. A brief discussion of other transport processes is given in Appendix B for completeness.

It is now clear to see that the perturbation can take effect only when the denominators in Eq. (14) are much greater than the numerators. In charge-2e SC, the energy constraint preserves that we just require the incident electron to be far away from the gap. However, in charge-4e SC, the loose constraint requires not only the incident electron but also the reflected holes should be far away from the gap. The perturbation would also break down at some diverging points as some reflected holes carry the opposite energy of the incident electron. However, these divergences can be compensated by considering the higher-order contributions. The maximum of $T^{(1)}_{A,4e}$ would happen when each reflected hole carries one-third of the energy of the incident electron, which is different from $T^{(1)}_{A,2e}$ that the energy of the reflected hole and the incident electron are usually equal [44].

Besides, we can see from Eq. (14) that the structure of $T^{(1)}_{A,4e}$ is similar to the $T^{(1)}_{A,2e}$. However, since $T^{(1)}_{A,4e} \propto E^{-6}$ and $T^{(1)}_{A,2e} \propto E^{-2}$ with E the incident energy, we find that they possess different energy dependence. Meanwhile, the square of coupling from z^2 to z^4 makes $T^{(1)}_{A,4e}$ change faster than $T^{(1)}_{A,2e}$ as z varies, which means that the conductance of charge-4e SC is more sensitive to the interface barriers than that of charge-2e SC.

IV. NONPERTURBATION IN SUPERCONDUCTIVITY: THE EQUATION OF MOTION METHOD

As the incident (reflected) energy stays below or near the gap, the breakdown of the perturbation expanded by superconducting pairing potential Δ implies that we should consider higher orders of Δ into the anomalous Green's function. One straightforward way is to expand the Andreev reflection coefficient to the lowest order of coupling $|t_c|^2$, which makes the nonequilibrium charge-4e anomalous Green's function $F_{k_1k_2k_3k_4}(0,t_2,t_3,t_4)$ regress to the equilibrium charge-4e anomalous Green's function $\delta_{kk_1}\delta_{kk_2}\delta_{kk_3}\delta_{kk_4}F_k(0,t_2,t_3,t_4)$. As the equilibrium Green's function of H_R can be solved exactly [27], for the convenience of future promotion to the weak coupling case, we introduce the equation of motion (EOM) for retarded charge-4e anomalous Green's functions.

A. EOM for equilibrium Green's function

We first solve the equilibrium charge-4e anomalous Green's functions of H_R at $t_c = 0$. By using Eq. (9) and the identity

$$1 = \sum_{(xyz)} \theta(0-t_x)\theta(t_x-t_y)\theta(t_y-t_z), \tag{15}$$

with (xyz) the permutation of (234), we rewrite the retarded charge-4e anomalous Green's function

$$\begin{aligned} F^r_k(0,t_2,t_3,t_4) &= \sum_{(xyz)} -i\mathscr{F}(\tilde{c}_{1k}(0),\tilde{c}_{xk}(t_x),\tilde{c}_{yk}(t_y),\tilde{c}_{zk}(t_z)) \\ &= \sum_{(xyz)} -iP(xyz)\theta(0-t_x)\theta(t_x-t_y)\theta(t_y-t_z) \\ &\quad \times \{[[\tilde{c}_{1k}(0),\tilde{c}_{xk}(t_x)\},\tilde{c}_{yk}(t_y)],\tilde{c}_{zk}(t_z)\}, \end{aligned} \tag{16}$$

where $P(xyz)$ is the sign of the permutation (xyz). $\tilde{c}_{1k},\tilde{c}_{2k},\tilde{c}_{3k},\tilde{c}_{4k}$ represent $c_{1k\uparrow},c_{1-k\downarrow},c_{2k\uparrow},c_{2-k\downarrow}$, respectively. Using the Fourier transform, we have

$$F^r_k(\omega_2,\omega_3,\omega_4) = \sum_{(xyz)} -i\mathscr{F}(\omega_x,\omega_y,\omega_z). \tag{17}$$

The EOM for $F^r_k(\mathscr{F})$ can then be obtained by considering the time derivative, with detailed derivation shown in Appendix C 1.

Recall the EOM for charge-2e anomalous Green's function, we note that the closure of the EOM relies on the commutation relation

$$\left[c_{1k\sigma},H^{2e}_{\rm SC}\right] = \Delta c^\dagger_{1-k-\sigma}, \quad \left[c^\dagger_{1-k-\sigma},H^{2e}_{\rm SC}\right] = \Delta c_{1k\sigma}, \tag{18}$$

which also shows the particle-hole symmetry in charge-2e SC. Similarly, for charge-4e SC, we have a commutation relation

$$\begin{aligned} \left[c_{1k\uparrow},H^{4e}_{\rm SC}\right] &= \Delta\, d^\dagger_{1k\uparrow}, \\ \left[d^\dagger_{1k\uparrow},H^{4e}_{\rm SC}\right] &= \Delta\, \xi_{1k\uparrow}c_{1k\uparrow}, \\ \left[\xi_{1k\uparrow}c_{1k\uparrow},H^{4e}_{\rm SC}\right] &= \Delta\, d^\dagger_{1k\uparrow}, \end{aligned} \tag{19}$$

guaranteeing the closure of the EOM. Here $d^\dagger_{1k\uparrow} = c^\dagger_{1-k\downarrow}c^\dagger_{2k\uparrow}c^\dagger_{2-k\downarrow}$ is the operator for charge-3e particles. $\xi_{1k\uparrow} = n_{1-k\downarrow}n_{2k\uparrow}n_{2-k\downarrow} + \bar{n}_{1-k\downarrow}\bar{n}_{2k\uparrow}\bar{n}_{2-k\downarrow}$ with $\bar{n} = 1-n$ shows the effect of occupation numbers to the excitations. Therefore, Eq. (19) expresses the particle-hole symmetry in charge-4e SC, where a charge-3e hole (particle) can be converted into a charge-e particle (hole) combining with its environment (described by ξ).

Equipped with this relation, we can write the EOM for charge-4e SC,

$$\begin{aligned}(\omega_z^- \mathbf{I}_3 - \mathcal{H})\mathbf{F} &= -i\mathbf{F}_1',\\ (\omega_{yz}^- \mathbf{I}_9 - \mathcal{H}_1)\mathbf{F}_1 &= -i\mathbf{F}_2',\\ (\omega_{xyz}^- \mathbf{I}_{27} - \mathcal{H}_2)\mathbf{F}_2 &= -i\mathbf{F}_0,\end{aligned} \tag{20}$$

with $\omega_z^- = \omega_z - i\eta$, $\omega_{yz}^- = \omega_y + \omega_z - i\eta$, $\omega_{xyz}^- = \omega_x + \omega_y + \omega_z - i\eta$ and η measuring the energy relaxation rate [42]. $\mathbf{I}_n$ is the $n \times n$ identity matrix. $\mathcal{H}, \mathcal{H}_{1,2}$ are the coefficient matrix and $\mathbf{F}, \mathbf{F}_{0,1,2}$ are the vectors containing charge-4e anomalous Green's functions with different number of time variables. The superscript "prime" means to select the first 3 (9) elements of $\mathbf{F}_1$ ($\mathbf{F}_2$). We leave the explicit form of $\mathcal{H}, \mathcal{H}_{1,2}$ and $\mathbf{F}, \mathbf{F}_{0,1,2}$ in Appendix C 2.

B. Equilibrium gap spectrum

Using Eq. (20), we show here the result of $\mathscr{F}$ at zero temperature,

$$\mathscr{F}(\omega_x, \omega_y, \omega_z) = i\Delta \frac{(\omega_z^- + 3\epsilon_k)(\omega_{yz}^- + 2\epsilon_k)(\omega_{xyz}^- + \epsilon_k) + \Delta^2(\omega_z^- + \omega_{yz}^- + \omega_{xyz}^- + 2\epsilon_k)}{\left[(\omega_z^- + \epsilon_k)^2 - E_k^2\right]\left[\omega_{yz}^{-2} - E_k^2\right]\left[(\omega_{xyz}^- - \epsilon_k)^2 - E_k^2\right](\omega_{xyz}^- + \epsilon_k)}, \tag{21}$$

with $E_k^2 = 4\epsilon_k^2 + \Delta^2$. This gives us more insights into the properties of charge-4e SC, especially the energy dispersion of quasiparticles, which can be obtained from poles of $\mathscr{F}$.

Similar to the charge-2e SC, the energy dispersion here also shows a gapped feature. However, we note that there are two types of gaps. As shown in Fig. 1, while $\pm E_k$ (shown as green lines) contribute a direct gap of Δ for the mixing of charge-2e particles (holes), $\pm\epsilon_k \pm E_k$ (shown as yellow and orange lines) contribute an indirect gap of $\Delta' = \sqrt{3}\Delta/2$ for the mixing of charge-e/-3e particles (holes). Similar to the charge-2e SC where the Andreev reflection can be enhanced at the gap, we will show below that the peaks of Andreev reflection in charge-4e SC are also related to those gaps.

C. EOM for nonequilibrium Green's function

We then consider adding the coupling of left leads into $\mathscr{F}$. In general, introducing the lead coupling would mix the momentum in the right side and make k not a good quantum number anymore. Besides, the nonzero voltage bias and the flowing current could regulate the behavior of quasiparticles through the occupation numbers [see in Eq. (19) and Appendix C 3]. These things would bring a lot of complexity to the description of the transport in charge-4e SC. Therefore, to capture the main characteristics of charge-4e AR, we consider below an approximation with weak coupling, which can also be achieved in experiments conveniently. At this point, the momentum mixture is weak as well as the current is relatively small so that we can see the lead coupling as an extra self-energy $\mathcal{E}$ to the charge-4e anomalous Green's function while keeping other things unchanged. This would correct the EOM in Eq. (20):

$$\begin{aligned}(\omega_z^- \mathbf{I}_3 - \mathcal{H} - \mathcal{E})\mathbf{F}_{\text{neq}} &= -i\mathbf{F}'_{1,\text{neq}},\\ (\omega_{yz}^- \mathbf{I}_9 - \mathcal{H}_1 - \mathcal{E}_1)\mathbf{F}_{1,\text{neq}} &= -i\mathbf{F}'_{2,\text{neq}},\\ (\omega_{xyz}^- \mathbf{I}_{27} - \mathcal{H}_2 - \mathcal{E}_2)\mathbf{F}_{2,\text{neq}} &= -i\mathbf{F}_0,\end{aligned} \tag{22}$$

with the subscript "neq" distinguishing the results here from those in the equilibrium case. We leave the explicit form of $\mathcal{E}, \mathcal{E}_{1,2}$ and discussion in Appendix C 3.

V. CHARGE-4e ANDREEV REFLECTION

Once we calculate the result of nonequilibrium charge-4e anomalous Green's functions through Eq. (22), it is straightforward to get the Andreev coefficient T_A by Eq. (11). Therefore, we now reach the stage to give the whole picture of the charge-4e AR, together with the calculated results of Andreev coefficient T_A. Unlike the charge-2e AR where the energy of the reflected hole is constrained to that of the incident electron, the loose constraint in charge-4e AR would give two additional energy degrees of freedom ω_2, ω_3 if we consider the incident electron with certain energy ω_1, leaving $\omega_4 = \omega_1 - \omega_2 - \omega_3$. Together with Eq. (13) which shows that the contribution of T_A to G_A is further constrained by Fermi distribution functions, for a given $\omega_1 = eV > 0$, we indeed only need to investigate the behavior of T_A in $-eV < \omega_{2,3,4} < 3eV$, which forms a triangle region in the ω_2-ω_3 plane [see in Fig. 2(a)]. Besides, the two types of gaps shown in Sec. IV would bring different "in-gap" areas to the energy triangle.

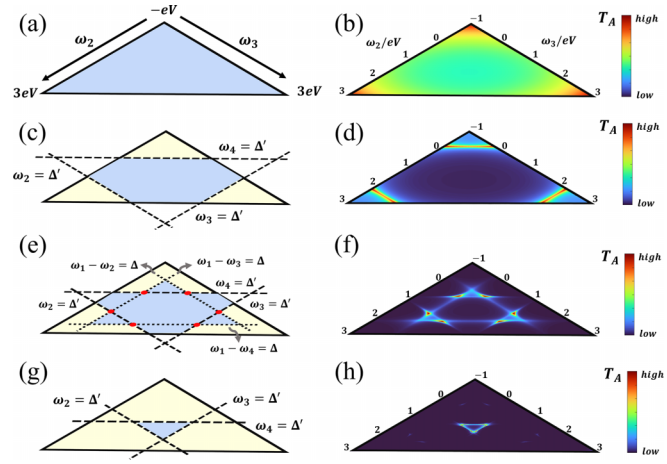

FIG. 2. Schematics of charge-4e Andreev reflection in ω_2-ω_3 energy plane (left column) with corresponding numerical results of T_A at $eV = 0.2, 0.4, 0.8, 1.8$ (from top to bottom of the right column) in the weak coupling case. While the blue regions denote the "in-gap" areas, we distinguish the separation lines induced by different gaps with different types of dotted lines. Moreover, we set $\Delta = 1$, $\rho_R = 1$, $\Gamma^L = 0.02$, and $\eta = 0.01$ in calculations [45].

We find that similar to the charge-2e AR, the charge-4e AR would also be enhanced around the energy gap as well as decay quickly outside the gap. Therefore, as ω_1 varies, the competing of these two gaps would change the "in-gap" area, which dominates the behavior of T_A and eventually influences the result of conductance G_A.

We begin with ω_1 being relatively small. As shown in Fig. 2(a), the whole energy triangle is inside the gap Δ' with all the incident (reflected) particles (holes) lying below the gap. Therefore, T_A stays stable with different energy but is slightly smaller in the center than around [see in Fig. 2(b)]. If we improve the strength of coupling, T_A would increase in the whole area. As ω_1 increases, some incident (reflected) particle (hole) would reach the gap Δ' where Andreev reflection gets enhanced. This requires that the maximum energy allowed to a single particle (hole) should satisfy $3eV \geqslant \Delta'$, giving a separation point $\omega_{c1} = \Delta'/3$. When $\omega_1 > \omega_{c1}$, the whole area would be separated by three lines $\omega_{2,3,4} = \Delta'$ located at the gap of charge-e/-3e particles [see in Fig. 2(c)]. In the weak coupling case, the strength of T_A concentrates on these gap lines [see in Fig. 2(d)]. As we improve the strength of coupling, those T_A belonging to the "in-gap" area [shown as the blue region in Fig. 2(c)] would also increase.

The further increasing of ω_1 allows two of the electrons can carry a total energy of Δ, touching the gap of charge-2e particles. This requires that $2eV \geqslant \Delta$, leading to another separation point $\omega_{c2} = \Delta/2$. When ω_1 exceeds ω_{c2}, a new set of three lines appears, with $\omega_1 - \omega_2 = \Delta$, $\omega_1 - \omega_3 = \Delta$, and $\omega_1 - \omega_4 = \Delta$ located at the gap of charge-2e particles. At this time, the "in-gap" area is encircled by six lines, showing a star of David structure [see in Fig. 2(e)]. In the weak coupling case, the peaks of T_A mainly focus on the crossover points of these lines [see in Fig. 2(f)]. The improvement of coupling would enhance the T_A in the whole area inside the star of David structure.

As ω_1 further increases across $\omega_{c3} = 2\Delta - \Delta'$, the "in-gap" area brought by Δ fully enters into the area brought by Δ'. As shown in Figs. 2(g) and 2(h), the maximum of T_A is then back to the position of Δ' gap. This "in-gap" area would eventually disappear as $\omega_1 \geqslant 3\Delta'$, leaving the maximum of T_A at the center of the energy triangle $\omega_2 = \omega_3 = \omega_4 = \omega_1/3$. This also matches Eq. (14) from the perturbation theory in the case of $\Delta \ll \omega_1$, showing the consistency of results provided by different methods.

VI. CONDUCTANCE

A. Conductance for Andreev reflection

Clarifying the behavior of T_A helps us understand the conductance of charge-4e SC, which can be measured in experiments. Applying Eq. (13), we first consider the conductance G_A contributed by the charge-4e AR [see in Fig. 3(a)]. From the numerical results, we find that the G_A possesses two major features. One is the conductance peak located at $\Delta' = \sqrt{3}\Delta/2$. The other is the emerging plateau beginning from $\Delta/2$.

When we consider increasing eV from zero, at first, G_A is contributed by those "in-gap" processes [shown in Figs. 2(a) and 2(b)]. In the weak coupling case, they are relatively small,

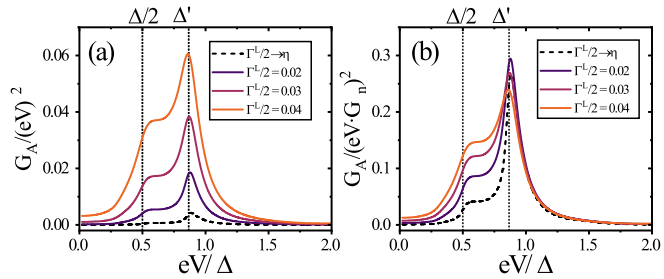

FIG. 3. (a) Conductance G_A contributed by the charge-4e AR with different coupling strength. (b) Conductance G_A in (a) is scaled by $G_n^2 \propto (\Gamma^L)^2$, which shows the consistency of decreasing coupling strength. We use dotted lines to highlight the major features in G_A. Besides, $G_n \approx 4\pi^2\rho_L\rho_R|t_c|^2 = 2\pi\rho_R\Gamma^L$ is the normal-state conductance in the weak coupling case [42,44]. We omit the unit e^2/h for conductance here and below and keep other parameters the same as those in Fig. 2 in calculations.

resulting in a near zero G_A. Once eV surpasses ω_{c1}, the emerging gap lines enhance the Andreev reflection [shown in Figs. 2(c) and 2(d)], causing the increasing of G_A before $eV = \Delta/2$ [see Fig. 3(a)]. The further increase of eV, however, turns the maximum of T_A from lines to points. The emerging plateau is then attributed to the fixed number of T_A peaks [shown in Figs. 2(e) and 2(f)]. Such peaks would reach their maximum at $eV = \Delta'$ [as shown in Fig. 3(a)], where all the participating electrons touch the gaps $\pm\Delta'$. We therefore get the G_A peak located at $eV = \Delta'$, which differs from the charge-2e AR that G_A is enhanced at Δ [44]. Apart from the peak, G_A decays. While in charge-2e AR, a quick $\Delta^2/[\Delta^2 - (eV)^2]$ behavior is presented [44], the asymmetric behavior here between $eV = \Delta'$ (especially when $\Gamma^L/2 \to \eta$) shows the slow decaying in charge-4e G_A due to the integral nature of it. Moreover, we compare our results with decreasing the coupling Γ^L, finding that the peak and plateau always appear at weak coupling cases. As the coupling decreases, the nonequilibrium Green's functions would regress to equilibrium Green's functions. Our results in Fig. 3(b) then indicate good consistency, with the small values of G_A being scaled by $G_n^2 \propto (\Gamma^L)^2$ at weak coupling cases.

B. Conductance for other transport processes

We then consider the contributions of other transport processes to the total conductance (see Appendix A 2 for the formulas used in numerical computation). Except for the quasiparticle tunneling process, the other transport processes can also be viewed as Andreev reflection with some of the reflected holes entering into the right leads. Similar to the charge-2e AR where an incident electron can be converted into a hole in the superconductor due to the "branch crossing" [42,44], we distinguish those processes by which side the reflected holes enter and use $T_{\alpha\beta\gamma}$, $G_{\alpha\beta\gamma}$, with $\alpha, \beta, \gamma = L, R$, to denote them (see Appendix A 2 for the detailed formulas.) Due to the coexistence of left-leaving holes and right-leaving holes, we find that they possess features both in Andreev reflection and normal tunneling with different types of quasiparticles. Therefore, we cannot simply attribute them to the

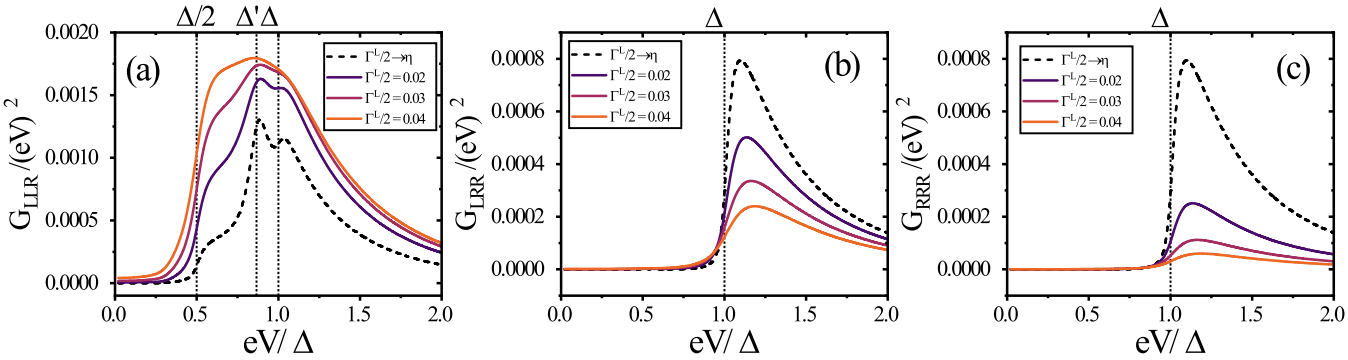

FIG. 4. Conductance contributed by the charge-4e AR with some reflected holes entering the right leads. (a)–(c) Show the conductance G_{LLR}, G_{LRR}, and G_{RRR}, respectively, with different coupling strengths. We use dotted lines to highlight major features in those conductances and keep other parameters the same as those in Fig. 2 in calculations.

transmission processes like what we usually do in charge-2e SC [32,38].

Figures 4(a)–4(c) show numerical results for the conductance G_{LLR}, G_{LRR}, and G_{RRR}, respectively. These processes contain both features in Andreev reflection and quasiparticle tunneling. While the emerging increase from $eV = \Delta/2$ and the peak at $eV = \Delta'$ is similar to that behavior of G_A, we attribute the peak at $eV = \Delta$ to the combination of charge-2e quasiparticles in the right leads. Note that the symmetry preserves that $G_{LLR} = G_{LRL} = G_{RLL}$ and $G_{LRR} = G_{RLR} = G_{RRL}$.

C. Total conductance

Finally, combining all the processes (including all Andreev reflections $G_{\alpha\beta\gamma}$ and the quasiparticle tunneling G_q) gives us the total differential conductance $G_{\rm tot}$. As shown in Fig. 5, in the weak coupling case, we have a U-shape curve of $G_{\rm tot}$.

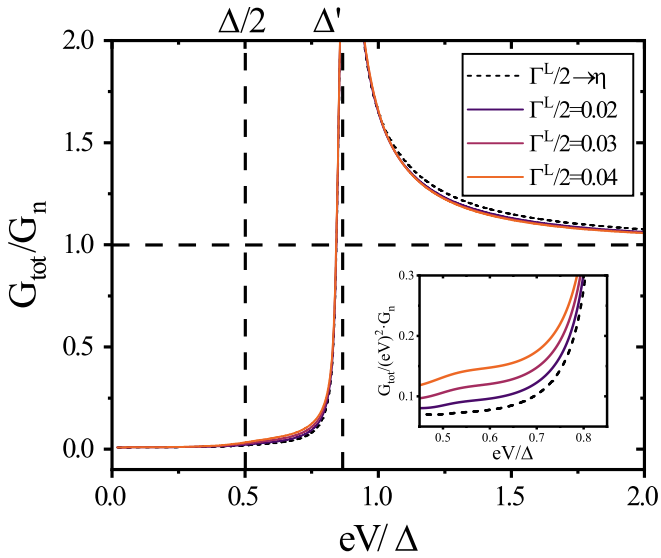

FIG. 5. Total conductance with different coupling strength. We use dashed lines to highlight the major features in $G_{\rm tot}$ and the insert shows detailed behavior of the plateau. Besides, we keep other parameters the same as those in Fig. 2 in calculations.

We also find the plateau beginning from $eV = \Delta/2$ as well as the conductance peak at $eV = \Delta'$. While the former is mainly contributed by G_A and $G_{LLR,LRL,RLL}$, the latter is mainly contributed by the divergence of the DOS in charge-4e SC [27]. As eV increases away from the gap, $G_{\rm tot}$ eventually tends to the normal-state conductance G_n, backing to the results in normal metal/normal metal junctions [42].

Moreover, it is beneficial to discuss the possible behaviors of $G_{\alpha\beta\gamma}$ in the strong coupling case. While in the weak coupling case, the increase of coupling would rise the height of the features at $\Delta/2$ and Δ' [see in Figs. 3(a) and 4(a)]. If we further improve the coupling, however, the increase of T_A in those "in-gap" areas would suppress the contribution in gap lines, eliminating the plateau feature. Therefore, when eV is close to zero, $G_A/(eV)^2 \approx (2/\pi^2)T_A$ is the constant proportional to the area of the energy triangle. As eV increases, the behavior of $G_A/(eV)^2$ would be proportional to the area of the "in-gap" region, and the total curve of G_A would show a V-shape behavior. Besides, to see the possible values of those conductances, we further consider an incident electron with energy E, the conservation of probability in charge-4e SC case requires that

$$1 = T_q(E) + R(E) + \sum_{\alpha\beta\gamma} \int'_{1234-i} T_{\alpha\beta\gamma}|_{\omega_i^e=E}, \tag{23}$$

where T_q is the tunneling coefficient and R is the reflection coefficient. $T_{\alpha\beta\gamma}$ are Andreev reflection coefficients with $T_{LLL} = T_A$. Due to the non-negativity of those coefficients, we have

$$0 \leqslant \int'_{1234-i} T_{\alpha\beta\gamma}|_{\omega_i^e=E} \leqslant 1, \tag{24}$$

which would give us an estimation for $G_{\alpha\beta\gamma}$. Note that here we do not involve Fermi distribution functions. This would extend the integral range to the whole energy plane and cause the result of the single integral in $G_{\alpha\beta\gamma}$ [see in Eqs. (13) and (A13)] less than that in Eq. (24). Therefore, we have

$$G_{\alpha\beta\gamma} \leqslant (n_{\alpha\beta\gamma} + 1)\frac{e^2}{h}, \tag{25}$$

with $n_{\alpha\beta\gamma}$ measuring the number of holes entering the left leads. We then expect to approach these values in some strong coupling cases, such as a possible maximum $4e^2/h$ peak at Δ' for the perfect charge-4e AR, differing from the maximum $2e^2/h$ peak of charge-2e AR [44].

VII. DISCUSSION AND CONCLUSIONS

The calculations above provide a comprehensive description of the charge-4e AR, from the transport formula to the picture of the behavior of T_A. Differing from the charge-2e SC, in charge-4e SC, the superconducting potential Δ introduces two types of gaps, an indirect gap of $\Delta' = \sqrt{3}\Delta/2$ for charge-e/3e quasiparticles and a direct gap of Δ for charge-2e quasiparticles. These two gaps compete with each other to decide the "in-gap" area for the T_A, thus introducing the conductance peak at $eV = \Delta'$ and the plateau beginning from $eV = \Delta/2$ at weak coupling case.

In experiments, these features can help us distinguish the charge-4e SC from the charge-2e SC. As the value of the superconducting potential usually remains unknown, it is hard to distinguish Δ' from Δ directly. Therefore, the existence of the plateau not only gives us direct evidence that differs from the conductance spectrum of charge-2e SC but also provides us a way to check the behavior of $\sqrt{3}$ as the ratio of the position of the gap and plateau. Besides, these behaviors also distinguish the charge-4e SC from two-gap charge-2e SC, as its conductance spectrum usually contains two peaks and irregular ratio of two gaps [46–50]. Moreover, if we can change the coupling continuously, like approaching the tip to the sample in STM experiments, the rising of the conductance inside the gap can alter the curve of the differential conductance from U shape and plateau to V shape, with a parabolic behavior near the center of the gap. This would give more hallmarks for experimental observation.

In summary, we investigate the Andreev reflection in a normal metal/charge-4e superconductor junction, which involves four particles due to the characteristics of quartet condensation. Using nonequilibrium Green's function method, we obtain a four-particle-type Landauer-Büttiker formula with generalized charge-4e anomalous Green's functions to describe this process. We then calculate and clarify the behavior of this process with various incident energy and show the conductance contributed by it. Our results can enrich the understanding of the transport with charge-4e SC and give more guidance for future experimental verifications.

ACKNOWLEDGMENTS

This work was financially supported by the National Natural Science Foundation of China (Grants No. 12374034 and No. 11921005), the Innovation Program for Quantum Science and Technology (Grant No. 2021ZD0302403), and the Strategic priority Research Program of Chinese Academy of Sciences (Grant No. XDB28000000). We also acknowledge the High-performance Computing Platform of Peking University for providing computational resources.

APPENDIX A: DERIVATION OF THE FORMULA FOR TRANSPORT PROCESSES IN NORMAL METAL/SUPERCONDUCTOR JUNCTIONS

In this Appendix, we derive the formula for transport processes in the normal metal/superconductor junction, with the superconducting side being either charge-2e superconductor or charge-4e superconductor.

1. Transport in charge-2e superconductivity

We first derive the transport formula in the case of charge-2e SC. To describe the Andreev reflection, we explicitly insert the coupling term of channel $1\downarrow$ into $G_{1\uparrow,k_1k_1'}(\tau_1,\tau_1')$. By using the Wick's theorem, we get

$$\begin{aligned}&[\text{part of } G_{1\uparrow,k_1k_1'}(\tau_1,\tau_1')]\\&= \int_c d\tau_2 d\tau_2' \sum_{k_2k_2'} F_{k_1k_2}(\tau_1,\tau_2)\,\Sigma_{1\downarrow}(\tau_2,\tau_2')\,F^{\dagger}_{k_2'k_1'}(\tau_2',\tau_1'),\end{aligned} \tag{A1}$$

with $F_{k_1k_2}(\tau_1,\tau_2)$ and $F^{\dagger}_{k_2'k_1'}(\tau_2',\tau_1')$ being the nonequilibrium anomalous Green's functions. $\Sigma_{1\downarrow}(\tau_2,\tau_2') = \sum_k |t_c|^2 g^h_{1\downarrow,k}(\tau_2,\tau_2')$ is the self-energy of coupling to channel $1\downarrow$ with $g^h_{1\downarrow,k}(\tau_2,\tau_2') = -i\langle a^{\dagger}_{1-k\downarrow}(\tau_2)a_{1-k\downarrow}(\tau_2')\rangle^c_0$ being the hole-type free Green's function in the decoupled system (i.e., when $t_c = 0$).

We then apply the analytic continuation [51] to get the less (greater) Green's function $G^{\lessgtr}_{1\uparrow,kk'}(\omega_1)$ as the Fourier transform of $G^{\lessgtr}_{1\uparrow,k_1k_1'}(t,0)$:

$$\begin{aligned}&[\text{part of } G^{<}_{1\uparrow,k_1k_1'}(\omega_1)]\\&= \sum_{k_2k_2'}\sum_{ss'} (-1)^P F^{+s}_{k_1k_2}(\omega_1)\,\Sigma^{ss'}_{1\downarrow}(\omega_1)\,F^{\dagger,s'-}_{k_2'k_1'}(\omega_1),\\&[\text{part of } G^{>}_{1\uparrow,k_1k_1'}(\omega_1)]\\&= \sum_{k_2k_2'}\sum_{ss'} (-1)^P F^{-s}_{k_1k_2}(\omega_1)\,\Sigma^{ss'}_{1\downarrow}(\omega_1)\,F^{\dagger,s'+}_{k_2'k_1'}(\omega_1),\end{aligned} \tag{A2}$$

with $s, s' = \pm$ being the branch index and P being the total number of "minus" branches among them. Besides, $F^{\pm\pm}_{k_1k_2}(\omega_1)$, $F^{\dagger,\pm\pm}_{k_2'k_1'}(\omega_1)$, and $\Sigma^{\pm\pm}_{1\downarrow}(\omega_1)$ are Fourier transforms of $F_{k_1k_2}(t^{\pm},0^{\pm})$, $F^{\dagger}_{k_2'k_1'}(t^{\pm},0^{\pm})$, and $\Sigma_{1\downarrow}(t^{\pm},0^{\pm})$, respectively. In order to get $G^{\lessgtr}_{1\uparrow,A}$, we need to select the less (greater) part $\Sigma^{\lessgtr}_{1\downarrow}$ from $\Sigma^{\pm\pm}_{1\downarrow}$. By using $\Sigma^{r}_{1\downarrow} = -\Sigma^{a}_{1\downarrow} = -i\Gamma^L/2$, $\Sigma^{<}_{1\downarrow} = if^h_{i\downarrow}\Gamma^L$, and $\Sigma^{>}_{1\downarrow} = -if^{\bar{h}}_{i\downarrow}\Gamma^L$ [52] we eventually obtain Eqs. (4) and (5) from Eq. (A2).

While Eq. (A2) contains the process of Andreev reflection, it should be emphasized that the rest parts of $\Sigma^{\pm\pm}_{1\downarrow}$ (i.e., $\Sigma^{r/a}_{1\downarrow}$) in Eq. (A2) also contributes to the other transport processes. Using the Keldysh equation [42]

$$\begin{aligned}\mathbf{G}^{\lessgtr} &= (1+\mathbf{G}^r\boldsymbol{\Sigma}^r)\mathbf{G}^{\lessgtr}_0(1+\boldsymbol{\Sigma}^a\mathbf{G}^a) + \mathbf{G}^r\boldsymbol{\Sigma}^{\lessgtr}\mathbf{G}^a\\&= \mathbf{G}^r\left[\mathbf{G}^{r-1}_0\mathbf{G}^{\lessgtr}_0\mathbf{G}^{a-1}_0 + \boldsymbol{\Sigma}^{\lessgtr}\right]\mathbf{G}^a,\end{aligned} \tag{A3}$$

the exact form of $G^{\lessgtr}_{1\uparrow,k_1k_1'}$ can be derived as [43,53,54] (omitting the energy variable ω_1)

$$\begin{aligned} G^{<}_{1\uparrow,k_1k_1'} &= \sum_{k_2k_2'} G^{r}_{1\uparrow,k_1k_2}\left[if^{e}_{1\uparrow}\Gamma^{L} + if\Gamma^{R}\delta_{k_2k_2'}\right]G^{a}_{1\uparrow,k_2'k_1'} \\ &\quad + F^{r}_{k_1k_2}\left[if^{h}_{1\downarrow}\Gamma^{L} + if\Gamma^{R}\delta_{k_2k_2'}\right]F^{\dagger,a}_{k_2'k_1'}, \\ G^{>}_{1\uparrow,k_1k_1'} &= \sum_{k_2k_2'} G^{r}_{1\uparrow,k_1k_2}\left[-i\bar{f}^{e}_{1\uparrow}\Gamma^{L} - i\bar{f}\Gamma^{R}\delta_{k_2k_2'}\right]G^{a}_{1\uparrow,k_2'k_1'} \\ &\quad + F^{r}_{k_1k_2}\left[-i\bar{f}^{h}_{1\downarrow}\Gamma^{L} - i\bar{f}\Gamma^{R}\delta_{k_2k_2'}\right]F^{\dagger,a}_{k_2'k_1'}, \end{aligned} \tag{A4}$$

where $\bar{f} = 1 - f$ and $f = f(\omega_1)$ is the Fermi distribution function in the right lead. $\Gamma^R = 2\eta$ measures the linewidth of the quasiparticles in the right lead [42]. Substituting Eq. (A4) into (3), we then get the transport formula for other transport processes.

One is the quasiparticle tunneling process, which contributes a current

$$I_{1\uparrow,q} = \frac{e}{h}\int \mathrm{d}\omega_1 (f^{e}_{1\uparrow} - f)\, T_q, \tag{A5}$$

where $T_q(\omega_1) = \Gamma^L\Gamma^R \sum_{k_1k_2k_1'} G^{r}_{1\uparrow,k_1k_2} G^{a}_{1\uparrow,k_2k_1'}$ is the tunneling coefficient.

The other is the Andreev process with the reflected hole entering the right lead, contributing a current

$$\begin{aligned} I_{1\uparrow,R} &= \frac{e}{h}\int \mathrm{d}\omega_1 \left(f^{e}_{1\uparrow}\bar{f} - \bar{f}^{e}_{1\uparrow} f\right) T_R \\ &= \frac{e}{h}\int \mathrm{d}\omega_1 \left(f^{e}_{1\uparrow} - f\right) T_R, \end{aligned} \tag{A6}$$

with $T_R(\omega_1) = \Gamma^L\Gamma^R \sum_{k_1k_2k_1'} F^{r}_{k_1k_2} F^{\dagger,a}_{k_2k_1'}$.

We usually do not distinguish these two processes and define the transmission current [38]

$$I_{1\uparrow,\mathrm{trans}} = \frac{e}{h}\int \mathrm{d}\omega_1 \left(f^{e}_{1\uparrow} - f\right) T_{\mathrm{trans}}, \tag{A7}$$

with transmission coefficient $T_{\mathrm{trans}} = T_q + T_R$. Together with Eq. (6), we have the total current

$$I_{1\uparrow,\mathrm{tot}} = I_{1\uparrow,A} + I_{1\uparrow,\mathrm{trans}}. \tag{A8}$$

2. Transport in charge-4*e* superconductivity

Similar to the charge-2*e* AR, the charge-4*e* AR can be described by inserting the coupling terms of the other three channels into $G_{1\uparrow,k_1k_1'}(\tau_1,\tau_1')$. Using the Wick's theorem, we get

$$\begin{aligned} &[\text{part of } G_{1\uparrow,k_1k_1'}(\tau_1,\tau_1')] \\ &= -\int_c d\tau_2 d\tau_3 d\tau_4 d\tau_2' d\tau_3' d\tau_4' \sum_{\substack{k_2k_3k_4\\ k_2'k_3'k_4'}} F_{k_1k_2k_3k_4}(\tau_1,\tau_2,\tau_3,\tau_4) \\ &\quad \times \Sigma_{1\downarrow}(\tau_2,\tau_2')\Sigma_{2\uparrow}(\tau_3,\tau_3') \\ &\quad \times \Sigma_{2\downarrow}(\tau_4,\tau_4') F^{\dagger}_{k_4'k_3'k_2'k_1'}(\tau_4',\tau_3',\tau_2',\tau_1'), \end{aligned} \tag{A9}$$

with $F_{k_1k_2k_3k_4}(\tau_1,\tau_2,\tau_3,\tau_4)$ and $F^{\dagger}_{k_4'k_3'k_2'k_1'}(\tau_4',\tau_3',\tau_2',\tau_1')$ being the nonequilibrium charge-4*e* anomalous Green's functions. $\Sigma_{i\sigma}(\tau,\tau') = \sum_k |t_c|^2 g^{h}_{i\sigma,k}(\tau,\tau')$ is self-energy of coupling to channel $i\sigma$ with $g^{h}_{i\sigma,k}(\tau,\tau') = -i\langle a^{\dagger}_{ik\sigma}(\tau) a_{ik\sigma}(\tau')\rangle^{c}_{0}$ being the hole-type free Green's function in the decoupled system (i.e., when $t_c = 0$).

We then apply the analytic continuation [51] and use the Fourier transform to get the less (greater) Green's functions

$$\begin{aligned} &[\text{part of } G^{<}_{1\uparrow,k_1k_1'}(\omega_1)] \\ &= -\int_{234} \sum_{\substack{k_2k_3k_4\\ k_2'k_3'k_4'}} \sum_{\substack{s_2s_3s_4\\ s_2's_3's_4'}} (-1)^{P} F^{+s_2s_3s_4}_{k_1k_2k_3k_4} \Sigma^{s_2s_2'}_{1\downarrow}(\omega_2) \\ &\quad \times \Sigma^{s_3s_3'}_{2\uparrow}(\omega_3)\Sigma^{s_4s_4'}_{2\downarrow}(\omega_4) F^{\dagger,s_4's_3's_2'-}_{k_4'k_3'k_2'k_1'}, \\ &[\text{part of } G^{>}_{1\uparrow,k_1k_1'}(\omega_1)] \\ &= -\int_{234} \sum_{\substack{k_2k_3k_4\\ k_2'k_3'k_4'}} \sum_{\substack{s_2s_3s_4\\ s_2's_3's_4'}} (-1)^{P} F^{-s_2s_3s_4}_{k_1k_2k_3k_4} \Sigma^{s_2s_2'}_{1\downarrow}(\omega_2) \\ &\quad \times \Sigma^{s_3s_3'}_{2\uparrow}(\omega_3)\Sigma^{s_4s_4'}_{2\downarrow}(\omega_4) F^{\dagger,s_4's_3's_2'+}_{k_4'k_3'k_2'k_1'}, \end{aligned} \tag{A10}$$

with $s_{2,3,4}, s_{2,3,4}' = \pm$ being the branch index and P denoting the total number of "minus" branches among them $F^{\pm\pm\pm\pm}_{k_1k_2k_3k_4} = F^{\pm\pm\pm\pm}_{k_1k_2k_3k_4}(\omega_2,\omega_3,\omega_4)$ and $F^{\dagger,\pm\pm\pm\pm}_{k_4'k_3'k_2'k_1'} = F^{\dagger,\pm\pm\pm\pm}_{k_4'k_3'k_2'k_1'}(\omega_4,\omega_3,\omega_2)$ are the Fourier transforms of $F_{k_1k_2k_3k_4}(0^{\pm},t_2^{\pm},t_3^{\pm},t_4^{\pm})$ and $F^{\dagger}_{k_4'k_3'k_2'k_1'}(t_4^{\pm},t_3^{\pm},t_2^{\pm},0^{\pm})$. $\Sigma^{\pm\pm}_{i\sigma}(\omega_j)$ is the Fourier transform of $\Sigma_{i\sigma}(t_j^{\pm},0^{\pm})$. To get $G^{\lessgtr}_{1\uparrow,A}$, we also need to select the less (greater) part $\Sigma^{\lessgtr}_{i\sigma}$ from the $\Sigma^{\pm\pm}_{i\sigma}$. With some simplification, we can get Eqs. (8) and (9) in the end.

Similar to the charge-2*e* SC, here we have extra processes contributing to the total conductance, including the quasiparticle tunneling and the other three types of Andreev processes. While the current $I_{1\uparrow,q}$ contributed by the quasiparticle tunneling has the same form as Eq. (A5), the formula for other transport processes can be generalized from Eq. (A6). We denote them as $I_{1\uparrow,\alpha\beta\gamma}$, with $\alpha,\beta,\gamma = L,R$ denoting which side the reflected holes enter, and set $I_{1\uparrow,LLL} = I_{1\uparrow,A}$. According to the number of reflected holes entering the right side, we have

$$\begin{aligned} I_{1\uparrow,LLR} &= \frac{e}{h}\int_{1234}' (f^{e}f^{e}f^{e}f - \bar{f}^{e}\bar{f}^{e}\bar{f}^{e}\bar{f})\, T_{LLR}, \\ I_{1\uparrow,LRR} &= \frac{e}{h}\int_{1234}' (f^{e}f^{e}ff - \bar{f}^{e}\bar{f}^{e}\bar{f}\bar{f})\, T_{LRR}, \\ I_{1\uparrow,RRR} &= \frac{e}{h}\int_{1234}' (f^{e}fff - \bar{f}^{e}\bar{f}\bar{f}\bar{f})\, T_{RRR}, \end{aligned} \tag{A11}$$

with

$$\begin{aligned} T_{LLR} &= (\Gamma^L)^3\Gamma^R \sum_{k_ik_j'} F^{r}_{1\uparrow,k_1k_2k_3k_4} F^{\dagger,a}_{1\uparrow,k_4k_3'k_2'k_1'}, \\ T_{LRR} &= (\Gamma^L)^2(\Gamma^R)^2 \sum_{k_ik_j'} F^{r}_{1\uparrow,k_1k_2k_3k_4} F^{\dagger,a}_{1\uparrow,k_4k_3k_2'k_1'}, \\ T_{RRR} &= \Gamma^L(\Gamma^R)^3 \sum_{k_ik_j'} F^{r}_{1\uparrow,k_1k_2k_3k_4} F^{\dagger,a}_{1\uparrow,k_4k_3k_2'k_1'}. \end{aligned} \tag{A12}$$

Others like $I_{1\uparrow,LRL}(T_{LRL})$, $I_{1\uparrow,RLR}(T_{RLR})$, etc., are analogous.

Therefore, we can measure their contributions to the conductance by $G_{\alpha\beta\gamma} = \partial I_{1\uparrow,\alpha\beta\gamma}/\partial V$,

$$G_{LLR} = \frac{e^2}{h}\sum_{i=1}^{3}\int'_{1234-i}(f^e f^e f + \bar{f}^e\bar{f}^e\bar{f})\,T_{LLR}|_{\omega_i^e=eV},$$
$$G_{LRR} = \frac{e^2}{h}\sum_{i=1}^{2}\int'_{1234-i}(f^e f f + \bar{f}^e\bar{f}\bar{f})\,T_{LRR}|_{\omega_i^e=eV},$$
$$G_{RRR} = \frac{e^2}{h}\int'_{1234-1}(f f f + \bar{f}\bar{f}\bar{f})\,T_{RRR}|_{\omega_1^e=eV}, \tag{A13}$$

assuming that all $T_{\alpha\beta\gamma}$ are independent of voltage V. Others are analogous. We then obtain the total current and conductance

$$I_{1\uparrow,\mathrm{tot}} = I_{1\uparrow,q} + \sum_{\alpha\beta\gamma} I_{1\uparrow,\alpha\beta\gamma},$$
$$G_{\mathrm{tot}} = G_q + \sum_{\alpha\beta\gamma} G_{\alpha\beta\gamma}, \tag{A14}$$

with $G_{LLL} = G_A$.

APPENDIX B: PERTURBATIVE EXPANSION FOR OTHER PROCESSES IN NORMAL METAL/CHARGE-4*e* SUPERCONDUCTOR JUNCTIONS

In this Appendix, we briefly discuss the perturbative expansion for other transport processes. The first one is the quasiparticle tunneling process, which is described by Eq. (A5). To calculate the nonequilibrium $G^{r/a}_{1\uparrow,k_1k_2}$, we begin with the Dyson equation [51]

$$G^{r/a}_{1\uparrow,k_1k_2}(\omega_1) = \delta_{k_1k_2}g^{r/a}_{1\uparrow,k_1}(\omega_1) + \sum_{k_1'k_2'} g^{r/a}_{1\uparrow,k_1}(\omega_1) \times \left[\delta_{k_1'k_2'}\Sigma_L^{r/a} + \Sigma^{r/a}_{1\uparrow,k_1'k_2'}(\omega_1)\right]G^{r/a}_{1\uparrow,k_2'k_2}(\omega_1), \tag{B1}$$

with $g_{1\uparrow,k}$ being the free Green's function. $\Sigma_L^{r/a} = \mp i\Gamma^L/2$ is the self-energy of coupling to channel $1\uparrow$ and $\Sigma^{r/a}_{1\uparrow,k_1'k_2'}(\omega_1)$ is the Fourier transform of the irreducible self-energy $\Sigma^{r/a}_{1\uparrow,k_1'k_2'}(t,0)$ containing the superconducting interaction and the coupling. Expanding $\Sigma_{1\uparrow,k_1'k_2'}(\tau,\tau')$ to the lowest order of Δ and applying the analytic continuation [51], we have

$$\Sigma^{(1)}_{1\uparrow,k_1'k_2'}(\tau,\tau') = -\Delta^2\mathcal{G}_{1\downarrow,k_1'k_2'}(\tau,\tau')\mathcal{G}_{2\uparrow,k_1'k_2'}(\tau,\tau') \times \mathcal{G}_{2\downarrow,k_1'k_2'}(\tau,\tau'),$$
$$\Sigma^{(1),\lessgtr}_{1\uparrow,k_1'k_2'}(t,t') = -\Delta^2\mathcal{G}^{\lessgtr}_{1\downarrow,k_1'k_2'}(t,t')\mathcal{G}^{\lessgtr}_{2\uparrow,k_1'k_2'}(t,t') \times \mathcal{G}^{\lessgtr}_{2\downarrow,k_1'k_2'}(t,t'), \tag{B2}$$

with

$$\mathcal{G}_{i\sigma,k_1'k_2'}(\tau,\tau') = \delta_{k_1'k_2'}g^h_{i\sigma,k_1'}(\tau,\tau') + \int_c d\tau_1 d\tau_1'\sum_k g^h_{i\sigma,k_1'}(\tau,\tau_1) \times \Sigma_{i\sigma}(\tau_1,\tau_1')\mathcal{G}_{i\sigma,kk_2'}(\tau_1',\tau'). \tag{B3}$$

Using [51] (omit the subscript for simplification)

$$\Sigma^{(1),r}(t,0) = \theta(t)[\Sigma^{(1),>}(t,0) - \Sigma^{(1),<}(t,0)],$$
$$\Sigma^{(1),a}(t,0) = \theta(-t)[\Sigma^{(1),<}(t,0) - \Sigma^{(1),>}(t,0)], \tag{B4}$$

the Fourier transform to $\Sigma^{(1),r/a}(\omega_1)$ would then lead to integrals over terms like $(f_\alpha f_\beta f_\gamma + \bar{f}_\alpha\bar{f}_\beta\bar{f}_\gamma)$, where $\alpha,\beta,\gamma = L,R$ denotes the Fermi distribution function in left (right) leads, as $\mathcal{G}^{\lessgtr}$ contains terms with $f_{L,R}$. This is consistent with the results in Ref. [5] and can be seen as the generalization to the nonequilibrium case. From this we can find that, in general, if we fix the energy of the incident electrons, the voltage bias would still affect T_q by changing the occupation numbers. This is consistent with the discussion in Sec. IV, showing the specific particle-hole symmetry in charge-4*e* SC.

As for the other three types of Andreev processes, the lowest-order expansions of $T_{\alpha\beta\gamma}$ can be expressed like (omitting the expressions of $A_{1,2,3}$ for simplification)

$$T^{(1)}_{LLR} = 4z^3v^2\frac{A_1(\omega_1^e,\omega_2^e,\omega_3^e,\omega_4^e,z_1)}{B(\omega_1^e,\omega_2^e,\omega_3^e,\omega_4^e)},$$
$$T^{(1)}_{LRR} = 4z^2v^2\frac{A_2(\omega_1^e,\omega_2^e,\omega_3^e,\omega_4^e,z_1)}{B(\omega_1^e,\omega_2^e,\omega_3^e,\omega_4^e)},$$
$$T^{(1)}_{RRR} = 4zv^2\frac{A_3(\omega_1^e,\omega_2^e,\omega_3^e,\omega_4^e,z_1)}{B(\omega_1^e,\omega_2^e,\omega_3^e,\omega_4^e)}, \tag{B5}$$

with $v = \Delta/\pi\rho_R$ and $z_1 = \pi\rho_R\Gamma^L/(2+\pi\rho_R\Gamma^L)$. Despite having different sensitivity to the coupling, the same form of the denominator of $T^{(1)}_{\alpha\beta\gamma}$ shows similar energy dependence. We can write it explicitly

$$B(\omega_1^e,\omega_2^e,\omega_3^e,\omega_4^e) = \prod_{i\neq j}(\omega_i^e - \omega_j^e)^2. \tag{B6}$$

Therefore, the perturbation breaks down when at least two of the incident electrons carry the same energy. In fact, it is these points that mainly contribute to $T_{\alpha\beta\gamma}$ and dominate the transmission processes.

APPENDIX C: THE EQUATION OF MOTION FOR RETARDED GREEN'S FUNCTIONS

In this Appendix, we derive the EOM for charge-4*e* anomalous Green's function.

1. The equation of motion for multitime retarded Green's function

According to Eq. (16), we begin with examining the time evolution of multitime retarded Green's function $\mathscr{F}$. For the convenience of future applications, we consider the general form of $\mathscr{F}(t_x,t_y,t_z)$,

$$\mathscr{F}(A(0),X(t_x),Y(t_y),Z(t_z)) = P(xyz)\theta(0-t_x)\theta(t_x-t_y)\theta(t_y-t_z) \times \{[[A(0),X(t_x)\},Y(t_y)],Z(t_z)\}, \tag{C1}$$

with operators A, X, Y, Z owning different times. The Fourier transform of $\mathscr{F}(t_x, t_y, t_z)$ can be written as

$$\begin{aligned}\mathscr{F}(\omega_x, \omega_y, \omega_z) &= \int \mathrm{d}t_x e^{i\omega_x t_x} \int \mathrm{d}t_y e^{i\omega_y t_y} \\ &\times \int \mathrm{d}t_z e^{i\omega_z t_z} \mathscr{F}(t_x, t_y, t_z) \\ &= \int_{-\infty}^{0} dt_x e^{i\omega_x t_x} \int_{-\infty}^{t_x} dt_y e^{i\omega_y t_y} \\ &\times \int_{-\infty}^{t_y} dt_z e^{i\omega_z t_z} \mathscr{F}(t_x, t_y, t_z). \end{aligned} \tag{C2}$$

We first consider the time derivative of t_z. Using the Heisenberg equation, we have

$$i\partial_{t_z}\mathscr{F}(t_x, t_y, t_z) = [\mathscr{F}, H_z](t_x, t_y, t_z), \tag{C3}$$

where $[\mathscr{F}, H_z] = \mathscr{F}(A(0), X(t_x), Y(t_y), [Z(t_z), H_{\mathrm{tot}}(t_z)])$. Notice that

$$\begin{aligned}&\int_{-\infty}^{t_y} dt_z e^{i\omega_z t_z}\, i\partial_{t_z}\mathscr{F}(t_x, t_y, t_z) \\ &= ie^{i\omega_z^- t_y}\mathscr{F}(t_x, t_y, t_y) + \omega_z^- \int_{-\infty}^{t_y} dt_z e^{i\omega_z t_z}\mathscr{F}(t_x, t_y, t_z).\end{aligned} \tag{C4}$$

The Fourier transform of Eq. (C2) then gives

$$\begin{aligned}&\omega_z^-\mathscr{F}(\omega_x, \omega_y, \omega_z) \\ &= -i\mathscr{F}_1(\omega_x, \omega_{yz}) + [\mathscr{F}, H_z](\omega_x, \omega_y, \omega_z).\end{aligned} \tag{C5}$$

Here $\mathscr{F}_1(\omega_x, \omega_{yz})$ is the Fourier transform of $\mathscr{F}(t_x, t_y, t_y)$ with $\omega_{yz} = \omega_y + \omega_z$. We note that in our calculations, $\omega_{x,y,z}$ are hole energies due to the selection of time variables that is opposite to the usual way. This also causes the $-i\eta$ which preserves the causality $0 > t_{x,y,z}$.

Repeatiung the above steps for t_x and t_y, we finally get a complete set of EOM,

$$\begin{aligned}\omega_z^-\mathscr{F}(\omega_x, \omega_y, \omega_z) &= -i\mathscr{F}_1(\omega_x, \omega_{yz}) + [\mathscr{F}, H_z](\omega_x, \omega_y, \omega_z), \\ \omega_{yz}^-\mathscr{F}_1(\omega_x, \omega_{yz}) &= -i\mathscr{F}_2(\omega_{xyz}) + [\mathscr{F}_1, H_y](\omega_x, \omega_{yz}), \\ \omega_{xyz}^-\mathscr{F}_2(\omega_{xyz}) &= -i\mathscr{F}_0 + [\mathscr{F}_2, H_x](\omega_{xyz}),\end{aligned} \tag{C6}$$

where $\mathscr{F}_0 = \mathscr{F}(A(0), X(0), Y(0), Z(0))$. $\mathscr{F}_2(\omega_{xyz})$, $[\mathscr{F}_1, H_y](\omega_x, \omega_{yz})$, and $[\mathscr{F}_2, H_x](\omega_{xyz})$ are the Fourier transforms of $\mathscr{F}(t_x, t_x, t_x)$, $[\mathscr{F}_1, H_y](t_x, t_y, t_y)$, and $[\mathscr{F}_2, H_x](t_x, t_x, t_x)$ with

$$\begin{aligned}[\mathscr{F}_1, H_y] &= \mathscr{F}(A(0), X(t_x), [Y(t_y), H_{tot}(t_y)], Z(t_y)) \\ &+ \mathscr{F}(A(0), X(t_x), Y(t_y), [Z(t_y), H_{tot}(t_y)]), \\ [\mathscr{F}_2, H_x] &= \mathscr{F}(A(0), [X(t_x), H_{tot}(t_x)], Y(t_x), Z(t_x)) \\ &+ \mathscr{F}(A(0), X(t_x), [Y(t_x), H_{tot}(t_x)], Z(t_x)) \\ &+ \mathscr{F}(A(0), X(t_x), Y(t_x), [Z(t_x), H_{tot}(t_x)]).\end{aligned} \tag{C7}$$

2. The equation of motion for equilibrium retarded Green's function

We here give the explicit form of the EOM to solve $\mathscr{F}(\omega_x, \omega_y, \omega_z)$. Using the EOM derived in Appendix C 1 and the commutation relations (19), we define $\mathbf{F}$, which is the Fourier transform of

$$\begin{pmatrix}\mathscr{F}(A(0), X_1(t_x), Y_1(t_y), Z_1(t_z)) \\ \mathscr{F}(A(0), X_1(t_x), Y_1(t_y), Z_2(t_z)) \\ \mathscr{F}(A(0), X_1(t_x), Y_1(t_y), Z_3(t_z))\end{pmatrix}, \tag{C8}$$

with $A = \tilde{c}_{1k}, X_1 = \tilde{c}_{xk}, Y_1 = \tilde{c}_{yk}$ and $Z_1 = \tilde{c}_{zk}, Z_2 = \tilde{d}_{zk}^\dagger$, $Z_3 = \tilde{\xi}_{zk}\tilde{c}_{zk}$. This leads to

$$(\omega_z^-\,\mathbf{I}_3 - \mathcal{H})\mathbf{F} = -i\mathbf{F}_1', \tag{C9}$$

with the coefficient matrix

$$\mathcal{H} = \begin{pmatrix}\epsilon_k & \Delta & 0 \\ 0 & -3\epsilon_k & \Delta \\ 0 & \Delta & \epsilon_k\end{pmatrix}, \tag{C10}$$

and $\mathbf{F}_1'$ being the Fourier transform of

$$\begin{pmatrix}\mathscr{F}(A(0), X_1(t_x), Y_1(t_y), Z_1(t_y)) \\ \mathscr{F}(A(0), X_1(t_x), Y_1(t_y), Z_2(t_y)) \\ \mathscr{F}(A(0), X_1(t_x), Y_1(t_y), Z_3(t_y))\end{pmatrix}. \tag{C11}$$

It then requires $\mathbf{F}_1'$ to solve $\mathbf{F}$. We thus define $\mathbf{F}_1$, in which the $(3i + j - 3)$ element is the Fourier transform of $\mathscr{F}(A(0), X_1(t_x), Y_i(t_y), Z_j(t_y))$, with $i, j = 1, 2, 3$. Here the definition of $Y_{1,2,3}$ is the same as $Z_{1,2,3}$ and we can get $\mathbf{F}_1'$ as the top three elements of $\mathbf{F}_1$.

Following the similar procedures, we can derive the EOM for $\mathbf{F}_1$,

$$(\omega_{yz}^-\,\mathbf{I}_9 - \mathcal{H}_1)\mathbf{F}_1 = -i\mathbf{F}_2', \tag{C12}$$

with the coefficient matrix

$$\begin{aligned}\mathcal{H}_1 &= \begin{pmatrix}\mathcal{H}_{11} & \Delta\mathbf{I}_3 & \mathbf{0} \\ \mathbf{0} & \mathcal{H}_{12} & \Delta\mathbf{I}_3 \\ \mathbf{0} & \Delta\mathbf{I}_3 & \mathcal{H}_{11}\end{pmatrix}, \\ \mathcal{H}_{11} &= \begin{pmatrix}2\epsilon_k & \Delta & 0 \\ 0 & -2\epsilon_k & \Delta \\ 0 & \Delta & 2\epsilon_k\end{pmatrix}, \\ \mathcal{H}_{12} &= \begin{pmatrix}-2\epsilon_k & \Delta & 0 \\ 0 & -6\epsilon_k & \Delta \\ 0 & \Delta & -2\epsilon_k\end{pmatrix}.\end{aligned} \tag{C13}$$

Besides, $\mathbf{F}_2'$ are the top nine elements in $\mathbf{F}_2$, in which the $(9i + 3j + k - 12)$ element is the Fourier transform of $\mathscr{F}(A(0), X_i(t_x), Y_j(t_x), Z_k(t_x))$, with $i, j, k = 1, 2, 3$. Here the definition of $X_{1,2,3}$ is the same as $Z_{1,2,3}$.

We then write the EOM for $\mathbf{F}_2$

$$(\omega_{xyz}^-\,\mathbf{I}_{27} - \mathcal{H}_2)\mathbf{F}_2 = -i\mathbf{F}_0, \tag{C14}$$

with $\mathcal{H}_2$ being the coefficient matrix similar to $\mathcal{H}, \mathcal{H}_1$. $\mathbf{F}_0$ is the vector with its $(9i + 3j + k - 12)$ element being $\mathscr{F}(A(0), X_i(0), Y_j(0), Z_k(0))$.

Since the value of $\mathbf{F}_0$ can be solved exactly [27], at zero temperature, we find that the nonzero terms in $\mathbf{F}_0$ are

$$\begin{aligned}&\mathscr{F}(A(0), X_2(0), Y_1(0), Z_1(0)) = 1, \\ &\mathscr{F}(A(0), X_2(0), Y_1(0), Z_3(0)) = 1, \\ &\mathscr{F}(A(0), X_3(0), Y_1(0), Z_2(0)) = -1.\end{aligned} \tag{C15}$$

This completes the whole set of EOM and we can solve $\mathscr{F}(\omega_x, \omega_y, \omega_z)$ as $\mathbf{F}(1)$.

3. The equation of motion for nonequilibrium retarded Green's function

Here we extend the EOM in Appendix C 2 to the nonequilibrium case with the coupling of the left normal metal lead and briefly discuss the complexity for transport in charge-4e SC. In charge-2e SC, the EOM for nonequilibrium Green's functions can still be closed with the help of commutation relations like

$$[c_{1k\sigma}, H_C] = t_c a_{1\sigma}, \quad [a_{1k\sigma}, H_C] = t_c c_{1\sigma}, \tag{C16}$$

where $a_{1\sigma} = \sum_k a_{1k\sigma}$ and $c_{1\sigma} = \sum_k c_{1k\sigma}$. However, the situation for charge-4e SC is much more complex, due to the commutation relations like

$$[d^\dagger_{1k\uparrow}, H_C] = -t_c\,(a^\dagger_{1\downarrow} c^\dagger_{2k\uparrow} c^\dagger_{2-k\downarrow} + c^\dagger_{1-k\downarrow} a^\dagger_{2\uparrow} c^\dagger_{2-k\downarrow} + c^\dagger_{1-k\downarrow} c^\dagger_{2k\uparrow} a^\dagger_{2\downarrow}), \tag{C17}$$

$$[\xi_{1k\uparrow} c_{1k\uparrow}, H_C] = t_c\,\xi_{1k\uparrow} a_{1\uparrow} + (j_{1-k\downarrow} \nu_{2k\uparrow,2-k\downarrow} + j_{2k\uparrow} \nu_{1-k\downarrow,2-k\downarrow} + j_{2-k\downarrow} \nu_{1-k\downarrow,2k\uparrow}) c_{1k\uparrow}, \tag{C18}$$

where $a^\dagger_{i\sigma} = \sum_k a^\dagger_{ik\sigma}$, $a_{i\sigma} = \sum_k a_{ik\sigma}$, $\nu_{ik,jk} = n_{ik} n_{jk} - \bar{n}_{ik} \bar{n}_{jk}$, and $j_{ik\sigma} = t_c \sum_{k'} (c^\dagger_{ik\sigma} a_{ik'\sigma} - a^\dagger_{ik'\sigma} c_{ik\sigma})$. Here Eq. (C17) describes the coupling between charge-3e particles and left leads, which would mix the momentum of three channels, and Eq. (C18) describes the effect that the occupation numbers in charge-4e SC would be affected by the appearance of the current.

To suppress these many-body correlation effects, we consider the approximation with weak coupling $|t_c|^2$, where the lead coupling only introduces an extra self-energy $\mathcal{E}$ to the charge-4e anomalous Green's function. This approximation is effective due to the dominant contribution of the diagonal term $\delta_{kk_1}\delta_{kk_2}\delta_{kk_3}\delta_{kk_4} F^r_{k_1k_2k_3k_4}$ to the summation $\sum_{k_i} F^r_{k_1k_2k_3k_4}$ as those momentum mixing terms are higher-order terms of $|t_c|^2$. Therefore, we have

$$\begin{aligned}(\omega_z^- \mathbf{I}_3 - \mathcal{H} - \mathcal{E})\mathbf{F}_{\rm neq} &= -i\mathbf{F}'_{1,\rm neq},\\ (\omega_{yz}^- \mathbf{I}_9 - \mathcal{H}_1 - \mathcal{E}_1)\mathbf{F}_{1,\rm neq} &= -i\mathbf{F}'_{2,\rm neq},\\ (\omega_{xyz}^- \mathbf{I}_{27} - \mathcal{H}_2 - \mathcal{E}_2)\mathbf{F}_{2,\rm neq} &= -i\mathbf{F}_0,\end{aligned} \tag{C19}$$

with

$$\mathcal{E} = \begin{pmatrix} i\Gamma^L/2 & 0 & 0 \\ 0 & 3i\Gamma^L/2 & 0 \\ 0 & 0 & i\Gamma^L/2 \end{pmatrix} \tag{C20}$$

and

$$\mathcal{E}_1 = \begin{pmatrix} \mathcal{E}_{11} & 0 & 0 \\ 0 & \mathcal{E}_{12} & 0 \\ 0 & 0 & \mathcal{E}_{11} \end{pmatrix},$$

$$\mathcal{E}_{11} = \begin{pmatrix} i\Gamma^L & 0 & 0 \\ 0 & 2i\Gamma^L & 0 \\ 0 & 0 & i\Gamma^L \end{pmatrix},$$

$$\mathcal{E}_{12} = \begin{pmatrix} 2i\Gamma^L & 0 & 0 \\ 0 & 3i\Gamma^L & 0 \\ 0 & 0 & 2i\Gamma^L \end{pmatrix}. \tag{C21}$$

$\mathcal{E}_2$ is similar to $\mathcal{E}, \mathcal{E}_1$. Notice that as we consider the coupling hardly altering the property of charge-4e SC, at zero temperature we still use the result of $\mathbf{F}_0$ in equilibrium. As the coupling is strengthened, not only the contribution of the momentum mixing terms needs to be considered but also the value of nonequilibrium $\mathbf{F}_0$ needs to be decided by some self-consistent method, which we would leave for future study.

[1] J. Bardeen, L. N. Cooper, and J. R. Schrieffer, Theory of superconductivity, Phys. Rev. **108**, 1175 (1957).

[2] G. Röpke, A. Schnell, P. Schuck, and P. Nozières, Four-particle condensate in strongly coupled fermion systems, Phys. Rev. Lett. **80**, 3177 (1998).

[3] C. Wu, Competing orders in one-dimensional spin- 3/2 fermionic systems, Phys. Rev. Lett. **95**, 266404 (2005).

[4] A. A. Aligia, A. P. Kampf, and J. Mannhart, Quartet formation at (100)/(110) interfaces of d -wave superconductors, Phys. Rev. Lett. **94**, 247004 (2005).

[5] T. Sogo, G. Röpke, and P. Schuck, Many-body approach for quartet condensation in strong coupling, Phys. Rev. C **81**, 064310 (2010).

[6] E.-G. Moon, Skyrmions with quadratic band touching fermions: A way to achieve charge 4e superconductivity, Phys. Rev. B **85**, 245123 (2012).

[7] R. M. Fernandes and L. Fu, Charge- 4e superconductivity from multicomponent nematic pairing: Application to twisted bilayer graphene, Phys. Rev. Lett. **127**, 047001 (2021).

[8] S.-K. Jian, Y. Huang, and H. Yao, Charge- 4e superconductivity from nematic superconductors in two and three dimensions, Phys. Rev. Lett. **127**, 227001 (2021).

[9] M. Hecker, R. Willa, J. Schmalian, and R. M. Fernandes, Cascade of vestigial orders in two-component superconductors: Nematic, ferromagnetic, s-wave charge-4e, and d-wave charge-4e states, Phys. Rev. B **107**, 224503 (2023).

[10] E. Berg, E. Fradkin, and S. A. Kivelson, Charge-4e superconductivity from pair-density-wave order in certain high-temperature superconductors, Nat. Phys. **5**, 830 (2009).

[11] E. Fradkin, S. A. Kivelson, and J. M. Tranquada, *Colloquium* : Theory of intertwined orders in high temperature superconductors, Rev. Mod. Phys. **87**, 457 (2015).

[12] V. Grinenko, D. Weston, F. Caglieris, C. Wuttke, C. Hess, T. Gottschall, I. Maccari, D. Gorbunov, S. Zherlitsyn, J. Wosnitza, A. Rydh, K. Kihou, C.-H. Lee, R. Sarkar, S. Dengre, J. Garaud, A. Charnukha, R. Hühne, K. Nielsch, B. Büchner *et al.*, State with spontaneously broken time-reversal symmetry above the superconducting phase transition, Nat. Phys. **17**, 1254 (2021).

[13] J. Ge, P. Wang, Y. Xing, Q. Yin, H. Lei, Z. Wang, and J. Wang, Evidence for multi-charge flux quantization in kagome superconductor ring devices, arXiv:2201.10352.

[14] D. F. Agterberg, M. Geracie, and H. Tsunetsugu, Conventional and charge-six superfluids from melting hexagonal Fulde-Ferrell-Larkin-Ovchinnikov phases in two dimensions, Phys. Rev. B **84**, 014513 (2011).

[15] S. Zhou and Z. Wang, Chern Fermi pocket, topological pair density wave, and charge-4e and charge-6e superconductivity in kagomé superconductors, Nat. Commun. **13**, 7288 (2022).

[16] J. Garaud and E. Babaev, Effective model and magnetic properties of the resistive electron quadrupling state, Phys. Rev. Lett. **129**, 087602 (2022).

[17] E. V. Herland, E. Babaev, and A. Sudbø, Phase transitions in a three dimensional U(1) × U(1) lattice London superconductor: Metallic superfluid and charge-4e superconducting states, Phys. Rev. B **82**, 134511 (2010).

[18] L. Radzihovsky, Fluctuations and phase transitions in Larkin-Ovchinnikov liquid-crystal states of a population-imbalanced resonant Fermi gas, Phys. Rev. A **84**, 023611 (2011).

[19] D. G. Barci and E. Fradkin, Role of nematic fluctuations in the thermal melting of pair-density-wave phases in two-dimensional superconductors, Phys. Rev. B **83**, 100509(R) (2011).

[20] C. Wang, Braiding statistics and classification of two-dimensional charge-2*m* superconductors, Phys. Rev. B **94**, 085130 (2016).

[21] E. Khalaf, P. Ledwith, and A. Vishwanath, Symmetry constraints on superconductivity in twisted bilayer graphene: Fractional vortices, 4*e* condensates, or nonunitary pairing, Phys. Rev. B **105**, 224508 (2022).

[22] J. B. Curtis, N. R. Poniatowski, Y. Xie, A. Yacoby, E. Demler, and P. Narang, Stabilizing fluctuating spin-triplet superconductivity in graphene via induced spin-orbit coupling, Phys. Rev. Lett. **130**, 196001 (2023).

[23] C. M. Varma and Z. Wang, Extended superconducting fluctuation region and 6*e* and 4*e* flux quantization in a kagome compound with a normal state of 3*Q* order, Phys. Rev. B **108**, 214516 (2023).

[24] P. Tarasewicz and D. Baran, Extension of the Fröhlich method to 4-fermion interactions, Phys. Rev. B **73**, 094524 (2006).

[25] Y.-F. Jiang, Z.-X. Li, S. A. Kivelson, and H. Yao, Charge-4e superconductors: A Majorana quantum Monte Carlo study, Phys. Rev. B **95**, 241103(R) (2017).

[26] N. V. Gnezdilov and Y. Wang, Solvable model for a charge-4e superconductor, Phys. Rev. B **106**, 094508 (2022).

[27] P. Li, K. Jiang, and J. Hu, Charge 4e superconductor: A wave-function approach, arXiv:2209.13905.

[28] C. W. J. Beenakker, Specular andreev reflection in graphene, Phys. Rev. Lett. **97**, 067007 (2006).

[29] M. Titov, M. Müller, and W. Belzig, Interaction-induced renormalization of andreev reflection, Phys. Rev. Lett. **97**, 237006 (2006).

[30] Z. Hou, Y. Xing, A.-M. Guo, and Q.-F. Sun, Crossed Andreev effects in two-dimensional quantum Hall systems, Phys. Rev. B **94**, 064516 (2016).

[31] Z. Hou and Q.-F. Sun, Double Andreev reflections in type-II Weyl semimetal-superconductor junctions, Phys. Rev. B **96**, 155305 (2017).

[32] P. Lv, Y.-F. Zhou, N.-X. Yang, and Q.-F. Sun, Magnetoanisotropic spin-triplet Andreev reflection in ferromagnet-Ising superconductor junctions, Phys. Rev. B **97**, 144501 (2018).

[33] J. C. Cuevas and M. Fogelström, Shot noise and multiple andreev reflections in d -wave superconductors, Phys. Rev. Lett. **89**, 227003 (2002).

[34] P. O. Sukhachov, F. von Oppen, and L. I. Glazman, Andreev reflection in scanning tunneling spectroscopy of unconventional superconductors, Phys. Rev. Lett. **130**, 216002 (2023).

[35] C. Lewandowski, É. Lantagne-Hurtubise, A. Thomson, S. Nadj-Perge, and J. Alicea, Andreev reflection spectroscopy in strongly paired superconductors, Phys. Rev. B **107**, L020502 (2023).

[36] A.-P. Jauho, N. S. Wingreen, and Y. Meir, Time-dependent transport in interacting and noninteracting resonant-tunneling systems, Phys. Rev. B **50**, 5528 (1994).

[37] Y.-B. Liu, J. Zhou, C. Wu, and F. Yang, Charge-4e superconductivity and chiral metal in 45°-twisted bilayer cuprates and related bilayers, Nat. Commun. **14**, 7926 (2023).

[38] Q.-F. Sun and X. C. Xie, Quantum transport through a graphene nanoribbon–superconductor junction, J. Phys.: Condens. Matter **21**, 344204 (2009).

[39] Y. Meir and N. S. Wingreen, Landauer formula for the current through an interacting electron region, Phys. Rev. Lett. **68**, 2512 (1992).

[40] Q.-f. Sun and X. C. Xie, Heat generation by electric current in mesoscopic devices, Phys. Rev. B **75**, 155306 (2007).

[41] S. G. Jakobs, M. Pletyukhov, and H. Schoeller, Properties of multi-particle Green's and vertex functions within Keldysh formalism, J. Phys. A: Math. Theor. **43**, 103001 (2010).

[42] J. C. Cuevas, A. Martín-Rodero, and A. Levy Yeyati, Hamiltonian approach to the transport properties of superconducting quantum point contacts, Phys. Rev. B **54**, 7366 (1996).

[43] Q.-F. Sun, J. Wang, and T.-H. Lin, Resonant Andreev reflection in a normal-metal–quantum-dot–superconductor system, Phys. Rev. B **59**, 3831 (1999).

[44] G. E. Blonder, M. Tinkham, and T. M. Klapwijk, Transition from metallic to tunneling regimes in superconducting microconstrictions: Excess current, charge imbalance, and supercurrent conversion, Phys. Rev. B **25**, 4515 (1982).

[45] S. B. Kaplan, C. C. Chi, D. N. Langenberg, J. J. Chang, S. Jafarey, and D. J. Scalapino, Quasiparticle and phonon lifetimes in superconductors, Phys. Rev. B **14**, 4854 (1976).

[46] P. Szabó, P. Samuely, J. Kačmarčík, T. Klein, J. Marcus, D. Fruchart, S. Miraglia, C. Marcenat, and A. G. M. Jansen, Evidence for two superconducting energy gaps in MgB_2 by point-contact spectroscopy, Phys. Rev. Lett. **87**, 137005 (2001).

[47] J.-X. Yin, Z. Wu, J.-H. Wang, Z.-Y. Ye, J. Gong, X.-Y. Hou, L. Shan, A. Li, X.-J. Liang, X.-X. Wu, J. Li, C.-S. Ting, Z.-Q. Wang, J.-P. Hu, P.-H. Hor, H. Ding, and S. H. Pan, Observation of a robust zero-energy bound state in iron-based superconductor Fe(Te,Se), Nat. Phys. **11**, 543 (2015).

[48] M. Ruby, B. W. Heinrich, J. I. Pascual, and K. J. Franke, Experimental demonstration of a two-band superconducting state for lead using scanning tunneling spectroscopy, Phys. Rev. Lett. **114**, 157001 (2015).

[49] J.-H. Ma, Z.-H. Pan, F. C. Niestemski, M. Neupane, Y.-M. Xu, P. Richard, K. Nakayama, T. Sato, T. Takahashi, H.-Q. Luo, L. Fang, H.-H. Wen, Z. Wang, H. Ding, and V. Madhavan, Coexistence of competing orders with two energy gaps in real and momentum space in the high temperature superconductor $Bi_2Sr_{2-x}La_xCuO_{6+\delta}$, Phys. Rev. Lett. **101**, 207002 (2008).

[50] H.-S. Xu, Y.-J. Yan, R. Yin, W. Xia, S. Fang, Z. Chen, Y. Li, W. Yang, Y. Guo, and D.-L. Feng, Multiband superconductivity with sign-preserving order parameter in kagome superconductor CsV_3Sb_5, Phys. Rev. Lett. **127**, 187004 (2021).

[51] H. Haug and A.-P. Jauho, *Quantum Kinetics in Transport and Optics of Semiconductors*, 2nd ed., Springer Series in Solid-State Sciences No. 123 (Springer, Berlin, 2008).

[52] J. Rammer and H. Smith, Quantum field-theoretical methods in transport theory of metals, Rev. Mod. Phys. **58**, 323 (1986).

[53] Q.-f. Sun, J. Wang, and T. h. Lin, Control of the supercurrent in a mesoscopic four-terminal Josephson junction, Phys. Rev. B **62**, 648 (2000).

[54] B. Wang and J. Wang, Statistical correlation for a three-terminal normal-metal–superconductor– superconductor hybrid system, Phys. Rev. B **67**, 014509 (2003).